

# Unveiling the organic contribution to the initial particle growth in 3-10 nm size range

Kewei Zhang<sup>1</sup>, Zhengning Xu<sup>1,2</sup>, Fei Zhang<sup>1,2</sup>, Zhibin Wang<sup>1,2,\*</sup>

5

<sup>1</sup>State Key Laboratory of Soil Pollution Control and Safety, Zhejiang Provincial Key Laboratory of Organic Pollution Process and Control, College of Environmental and Resource Sciences, Zhejiang University, Hangzhou 310058, China

<sup>2</sup>ZJU-Hangzhou Global Scientific and Technological Innovation Center, Zhejiang University, Hangzhou 311200, China

Correspondence to: Zhibin Wang ([wangzhibin@zju.edu.cn](mailto:wangzhibin@zju.edu.cn))

## 10 Abstract

Organic compounds play an important role in atmospheric particle initial growth along with sulfuric acid (SA). However, the detailed composition of newly formed particles remains limited due to analytical challenges. In this study, we conducted flow tube experiments to investigate the nanoparticle growth processes of SA and oxygenated organic molecules (OOMs, from  $\alpha$ -pinene oxidation) system. Utilizing a custom-built scanning flow condensation particle counter (SF-CPC), we report, for the first time, size-resolved measurements of the hygroscopicity parameter ( $\kappa$ ) and organic mass fraction ( $f_{\text{org}}$ ) for particles in the 3-10 nm size range within this atmospherically relevant system. The hygroscopicity of SA decreased 49% as particle size increased (from  $0.413 \pm 0.011$  at 3 nm to  $0.209 \pm 0.004$  at 10 nm) and declined by up to 18% with increasing RH, which may be explained by hydration effects. In contrast, the  $\kappa$  values of OOMs increased with RH by as much as 57%, potentially involving changes in oxidation product. Size-resolved  $f_{\text{org}}$  revealed that larger particles contained a greater proportion of organics, indicating OOMs contribute more significantly to growth at larger sizes. Moreover, elevated humidity enhanced the organic contribution to particle growth by up to 81%. Compared to 3-5 nm, this enhancement was more pronounced for 5-10 nm particles associated with the incorporation of increased yields of more volatile oxidation products and Kelvin effect. These valuable information on hygroscopicity and chemical composition of 3-10 nm particles during new particle formation and subsequent growth could further the understanding of related atmospheric mechanisms.

15

20

## 25 1 Introduction

Atmospheric new particle formation (NPF) is a widely observed phenomenon (Du et al., 2024; Kulmala et al., 2014) in which low-volatility gas-phase oxidation products nucleate to form aerosol particles (Lee et al., 2019). These newly formed particles can grow to become cloud condensation nuclei (CCN), potentially contributing 30-70% of atmospheric CCN populations (Ren et al., 2021; Sun et al., 2024). The chemical composition of nucleating clusters and growing particles plays  
30 a fundamental role in determining both particle formation mechanisms and subsequent growth processes (Kirkby et al., 2023). However, the chemical information of the cluster and particles are still not well understood (Zhang et al., 2012; Zhao et al., 2024).

To date, the condensation of low volatility vapours, like sulfuric acid (SA) or oxidized organic compounds, is recognized as a primary mechanism driving cluster formation and particle growth (Stolzenburg et al., 2018, 2020). SA, in particular, is a  
35 key gas-phase precursor involved in the nucleation of atmospheric aerosol particles (Kulmala, 2003; Sipilä et al., 2010). Field observations (Kulmala et al., 2013; Wang et al., 2011; Yao et al., 2018; Zhang et al., 2009) and laboratory experiments (Dunne et al., 2016; Kirkby et al., 2023; Sipilä et al., 2010) demonstrate it also contributes to initial growth. But SA only contributes 10%-50% exceeding 3 nm (Stolzenburg et al., 2023), which indicates that SA alone rarely dominates nanoparticle growth in the atmosphere (Kuang et al., 2010). In addition,  $\alpha$ -pinene oxidation products contribute to the growth of newly formed  
40 particles (Ehn et al., 2014; Tröstl et al., 2016). Atmospheric organic vapors play a crucial role in particle formation and growth (Kirkby et al., 2016; Riccobono et al., 2014; Zhang et al., 2004), with organic compounds potentially accounting for a substantial fraction (20-90%) of submicron particle mass (Jimenez et al., 2009). And the contribution of organic species to particle growth was found to increase with particle size (Bianchi et al., 2019; Riccobono et al., 2012; Riipinen et al., 2012). However, quantitative analysis of SA or organic mass fractions in 3-10 nm particles remains challenging due to instrumental  
45 limitations in measuring chemical composition (Smith et al., 2021; Zhang et al., 2022).

Several techniques have been developed to address this measurement gap. The thermal desorption chemical ionization mass spectrometer (TDCIMS) could characterize particle composition down to 8 nm in field (Li et al., 2021), though requiring extended sampling periods (10-30 minutes). Keskinen et al. (2013) estimated the organic fraction in sub-2 nm using atmospheric pressure interface time-of-flight (API-TOF) mass spectrometer. To break the limitation of insufficient ion  
50 concentration, alternative approaches utilizing advanced condensation particle counters (CPCs) provided qualitative assessments of organic contributions (Kangasluoma et al., 2014; Kulmala et al., 2007; O'Dowd et al., 2002), by exploiting the inherently high number concentration of nucleation-mode particles. The nano cloud condensation nuclei counter (nano-CCNC) could further provide semi-quantitative information by applying the linear relationship between hygroscopicity parameter ( $\kappa$ ) and organic mass fraction ( $f_{\text{org}}$ ) down to 2.5 nm (Wang et al., 2015). Though its stabilization period ( $\sim 2$  minutes for a single supersaturation) limits applicability to rapidly growing newly formed particles (e.g.,  $35.7 \text{ nm h}^{-1}$  in urban Shanghai, Xiao et al., 2015). More recently, the scanning flow condensation particle counter (SFCPC) has demonstrated capability for the  $\kappa$ - $f_{\text{org}}$

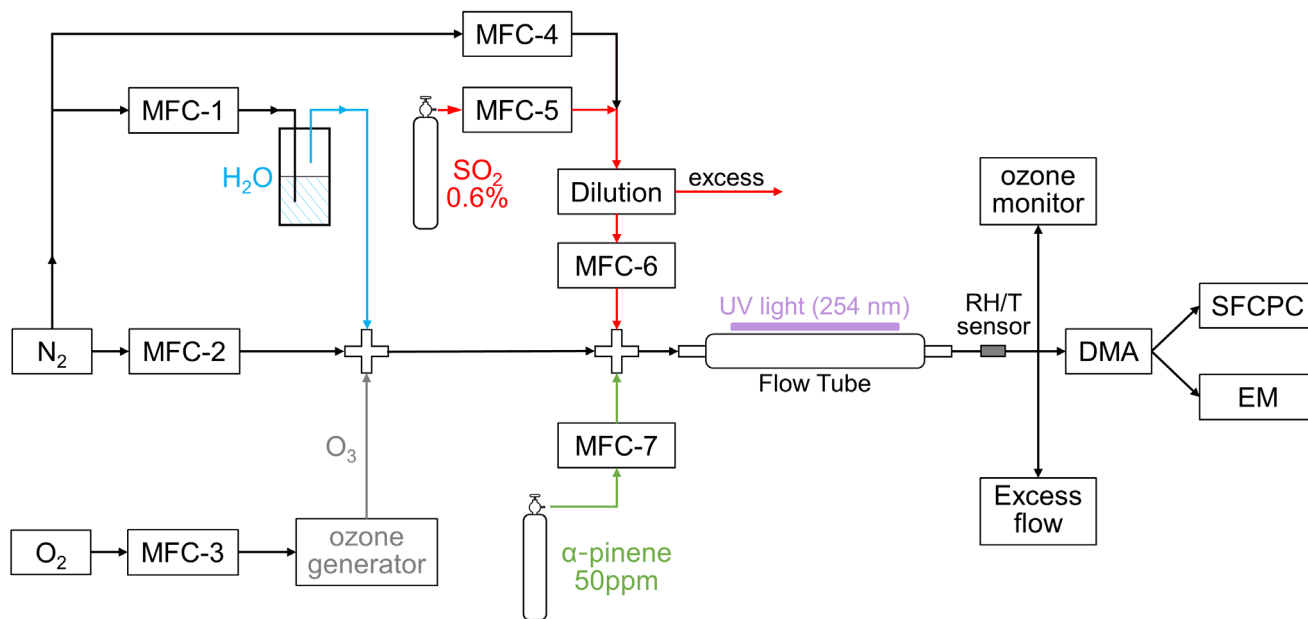
relationship by achieving supersaturation adjustments within  $\sim 2$  seconds through flow rate modulation (Zhang et al., 2023), making it particularly suitable for organic fraction determination in 3-10 nm.

In this study, we conducted a series of laboratory nucleation and growth experiments using a custom-built flow tube reactor.  $\text{SO}_2$  and  $\alpha$ -pinene were employed as gas-phase precursors to generate SA and organics (OOMs, oxygenated organic molecules), respectively. Experiments were performed under purely inorganic, purely organic, and mixed precursor conditions with varying  $[\alpha\text{-pinene}]/[\text{SO}_2]$  ratios, across a wide RH range (20%-80%). We first measured the  $\kappa$  values of 3-10 nm particles formed from the oxidation products through SFCPC. Then our analysis established size-resolved linear relationships between  $\kappa$  and  $f_{\text{org}}$  for SA-OOMs mixed particles, enabling quantitative determination of organic contributions. Furthermore, we systematically examined the effects of particle size, gas precursor concentration ratio, and humidity on both particle hygroscopicity and organic contribution. Based on these experimental results, this study aims to quantitatively investigate the distinct roles of sulfuric acid and oxygenated organics during nanoparticle growth, and to clarify how environmental conditions modulate the chemical composition and water uptake of sub-10 nm particles.

## 2 Materials and methods

### 2.1 Experimental set-up

A custom-built flow tube reactor was used to perform a series of laboratory studies on nucleation and growth. This flow tube consisted of a 25 cm long  $\times$  1 cm i.d. quartz tube (19.6 mL in volume) fitted with stainless steel adapter on each end. The entrance was coupled with two union cross in line to introduce gas precursors. As shown in Figure 1, the water vapor generated by passing  $\text{N}_2$  through water and  $\text{O}_3$  from a UVP ozone generator (model SOG-2, Analytik Jena US) were introduced into the main gas flow in the first union cross. The SA and OOMs in all experiments were generated from  $\text{SO}_2$  and  $\alpha$ -pinene. These precursors were diluted from a gas cylinder containing 0.6%  $\text{SO}_2$  and obtained from a gas cylinder with 50 ppmv  $\alpha$ -pinene, respectively. The carrier flow, water vapor,  $\text{O}_3$ ,  $\text{SO}_2$  and  $\alpha$ -pinene were mixed in the second union cross and then introduced into flow tube reactor. To initiate photolysis reactions in the system, a UV lamp (model 11SC-1, Analytik Jena US) with a length of 5.38 cm was installed at the entrance of the quartz tube, emitting ultraviolet light at a wavelength of 254 nm. At the exit of flow tube reactor, the temperature and RH were measured by a humidity sensor (model SHT85, Sensirion) with precision of  $\pm 1.5\%$ . The  $\text{O}_3$  concentration was monitored by an ozone analyser (model 49i, Thermo Fisher Scientific). The concentrations of other gaseous precursors were derived from their mixing ratios, and the molecular composition of the flow tube products was not directly measured in this study.



85 **Figure 1. Schematic of the flow tube reactor and experimental setup. Precursors (SO<sub>2</sub>,  $\alpha$ -pinene, O<sub>3</sub> and H<sub>2</sub>O) were introduced into the flow tube at a total flow rate of  $\sim 3$  L min<sup>-1</sup>. SO<sub>2</sub> and  $\alpha$ -pinene were subsequently oxidized by O<sub>3</sub> under UV irradiation (254 nm). The resulting oxidation products were classified using a nano-DMA, with particle hygroscopicity and organic content characterized by SFCPC and EM.**

SA and OOMs was used in this work to represent inorganic and organic components in atmosphere respectively. For pure  
 90 inorganic experimental groups, H<sub>2</sub>SO<sub>4</sub> was generated in situ via the reaction of OH radicals with SO<sub>2</sub> in the presence of water  
 vapor. When the SO<sub>2</sub>, O<sub>3</sub> and H<sub>2</sub>O were mixed and introduced into the flow tube reactor, O<sub>3</sub> underwent photolysis to produce  
 O(<sup>1</sup>D) atoms, which then react with water vapor to generate OH radicals. These OH radicals interact with SO<sub>2</sub>, forming the  
 HOSO<sub>2</sub> adduct, which subsequently decomposed to produce SO<sub>3</sub> and HO<sub>2</sub> (Jayne et al., 1997; Lovejoy et al., 1996). In the  
 reaction of SO<sub>3</sub> with water vapor, two H<sub>2</sub>O molecules or one H<sub>2</sub>O dimer per SO<sub>3</sub> molecule were required, ultimately resulting  
 95 in the formation of H<sub>2</sub>SO<sub>4</sub> (Berndt et al., 2005). For pure organic experimental groups, OOMs were produced from organic  
 peroxides formed from oxidation reactions of  $\alpha$ -pinene (Kirkby et al., 2016; Lee et al., 2019).  $\alpha$ -pinene was exposed to ozone  
 and also to hydroxyl radicals (OH $\cdot$ ) due to the unavoidable production of OH $\cdot$  from ozone photolysis and secondary reactions.  
 Although detailed molecular composition information could not be obtained in our work, the ozonolysis pathway is generally  
 understood to proceed via Criegee intermediates, leading to various peroxy radicals and subsequent low-volatility products  
 100 (Iyer et al., 2021; Yang et al., 2025). Similarly, OH-initiated oxidation proceeds mainly via OH $\cdot$  addition, forming peroxy  
 radicals that further react to produce condensable organic species (Berndt et al., 2016; Kang et al., 2025). While the present  
 study did not estimate the OH $\cdot$  concentration and further elucidate specific mechanistic pathways, this simplification is justified  
 because, to the best of our knowledge, no existing studies have clearly demonstrated significant differences in the hygroscopic  
 performance of pure OOMs derived from different  $\alpha$ -pinene oxidation pathways.

105 The SO<sub>2</sub> and  $\alpha$ -pinene concentration in experiments were regulated by setting the mixing ratio of SO<sub>2</sub> flow rate and  $\alpha$ -  
pinene flow rate to the total flow rate. The total flow rate was 3000 mL min<sup>-1</sup>, and the residence time in flow tube reactor was  
about 0.4 s. The all flow rates in this flow tube reactor were set by mass flow controllers (MFCs; MFC. 1-4, model GT130D,  
Gas Tool Instruments Co., Ltd.; MFC. 5-7, model Sevenstar CS200, NAURA Technology Group Co., Ltd.). The conditions  
of 24 experimental groups conducted to research the organic contribution to new formed particles in the initial growth stage  
110 were summarized in Table S1. To research the RH impacts to the initial growth process, the experiments were divided to four  
series conducted under RH 20%, 40%, 60% and 80%. For pure inorganic (Exp. A) and mixture groups (Exp. C-F), the  
concentration of SO<sub>2</sub> was set as a constant value and the concentration of  $\alpha$ -pinene was regulated based on the [ $\alpha$ -pinene]/[SO<sub>2</sub>]  
(concentration ratio of gas precursors  $\alpha$ -pinene and SO<sub>2</sub>, 0.1-1). The pure organic experiments (Exp. B) were conducted with  
much higher concentration than that in mixture experimental groups to generate sufficient 3-10 nm particles (number  
115 concentration larger than 1000 # cm<sup>-3</sup>). The temperature in all experiments was around 28 °C when the reaction was stable. O<sub>3</sub>  
concentration obtained by Ozone monitor was ~200 ppb with a regulable O<sub>2</sub> flow rate.

## 2.2 Determination of $\kappa$

The hygroscopicity of nanoparticles was measured with a custom-designed SFCPC. The setup of SFCPC system has been  
described previously (Zhang et al., 2023), and only a brief summary is presented here. The aerosol particles were passed  
120 through a neutralizer (X-ray, TSI model 3080), and a nano-differential mobility analyzer (nano-DMA, TSI model 3086) was  
used to select charged monodisperse particles in diameter range of 3-10 nm (with intervals of 0.2 nm in the 3-4 nm range and  
intervals of 0.5 nm in the 4-10 nm range). Considering the negligible probability of double-charge for particles below 20 nm  
(Fuchs, 1963; Wiedensohler et al., 1986; Wiedensohler and Fissan, 1988), no double-charge correction was applied in the  
studied size range. SFCPC, which was improved from a water-based condensation particle counter (WCPC, TSI model 3788)  
125 and could change the supersaturation fast by altering the sample flow, was deployed to count the activated particle  
concentration ( $N$ ). And an electrometer (EM, TSI model 3068B) was operated in parallel to measure the total particle  
concentration ( $N_{\text{total}}$ ), where the counting efficiency of sampled particles ( $f_{\text{count}}$ ) in different supersaturation ( $S$ ) conditions could  
be obtained by  $N/N_{\text{total}}$ .  $S$  distributions of SFCPC were calibrated by tungsten oxides (WO<sub>x</sub>) particles generated from a WO<sub>x</sub>  
generator (Model 7.860, Grimm Aerosol Technik; Steiner, 2006), and twelve  $S$  conditions were setup to meet the requirements  
130 of  $\kappa$  value measurements. The effective  $S$  ranged from 7.7% to 73.1%, a sufficiently broad range to activate the SA and OOMs  
corresponding  $f_{\text{count}}$  in 20%-80%. For the measurement part, particles from flow tube reactor were selected with discrete  
diameters and the  $S$  could be calculated through the measured  $f_{\text{count}}$ . Then the  $\kappa$  values could be obtained from dry diameter  
( $D_d$ ) and its corresponding  $S$  based on  $\kappa$ -Köhler equation (Petters and Kreidenweis, 2007). The equation was applied following  
Equation 2 in Zhang et al. (2023), in which the surface tension of water (0.072 N m<sup>-1</sup>) was used.

## 135 2.3 Determination of $f_{\text{org}}$

The linear relationship between chemical composition and hygroscopicity of CCN sized particles has been found both in  
laboratory experiments and field measurements (Dusek et al., 2010; Pöhlker et al., 2023; Vogel et al., 2016; Zhou et al., 2024).

Our previous work extended the linear relationship between  $\kappa$  and  $f_{\text{org}}$  to 3-10 nm size range for AS and levoglucosan/sucrose mixed particles, which were generated via Electrospray from solutions with known mixing ratios (Wang et al., 2015; Zhang et al., 2023). Zhang et al. (2025) assessed the uncertainty arising from the dependence of  $\kappa$  on particle size, also based on Electrospray-generated particles (AS and *cis*-pinonic acid). In this work, we introduced  $\kappa$ - $f_{\text{org}}$  linear relationship into the mixing products from flow tube—a setup designed to simulate atmospheric processes—in order to explore the organic content in the particulate phase. Furthermore, we established size-resolved  $\kappa$ - $f_{\text{org}}$  linear relationship to eliminate the mentioned uncertainty. The application of the  $\kappa$ - $f_{\text{org}}$  linear relationship relies on the assumption of ideal internal mixing within the particles. Under our experimental conditions, for in situ freshly formed 3-10 nm particles, the characteristic mixing times are short, and organic-inorganic mixtures are likely to remain liquid and well-mixed (Cheng et al., 2015). Therefore, the ideal internal mixing assumption is reasonable. For SA-OOMs mixture, we use the  $\kappa$  values of pure organic (OOMs) and inorganic (SA) experiment groups to represent the hygroscopicity of the organic and inorganic component in the mixture particles, respectively. Although the organic and inorganic components in mixture may not be identical to those in pure organic and inorganic particles of the same size under the same RH due to the potential change of oxidation processes, this simplification is a necessary given the current inability to directly measure the composition and component-specific hygroscopicity of particles in the 3-10 nm size range. To further reduce uncertainties associated with the linear relationship, the  $\kappa$  values of pure organic and inorganic particles were taken from the fitted lines to serve as a reference baseline, as shown in Figure S1. Based on the size-resolved  $\kappa$ - $f_{\text{org}}$  linear relationship (colored solid lines) and the measured  $\kappa$  values (grey dashed line) of the SA-OOMs mixture, the corresponding  $f_{\text{org}}$  values (colored dashed lines) for particles generated in the flow tube reactor were derived using Eq. 1:

$$f_{\text{org}} = \frac{\kappa - \kappa_{\text{inorg}}}{\kappa_{\text{org}} - \kappa_{\text{inorg}}} \times 100\% \quad (1)$$

where  $f_{\text{org}}$  and  $\kappa_{\text{org}}$  is the mass fraction and hygroscopicity of pure organics (OOMs in this work), respectively;  $\kappa_{\text{inorg}}$  is the hygroscopicity of pure inorganic component (SA in this work);  $\kappa$  is the hygroscopicity of the measured particles nucleation and growth process in flow tube reactor.

## 160 3 Results and discussion

### 3.1 Hygroscopicity

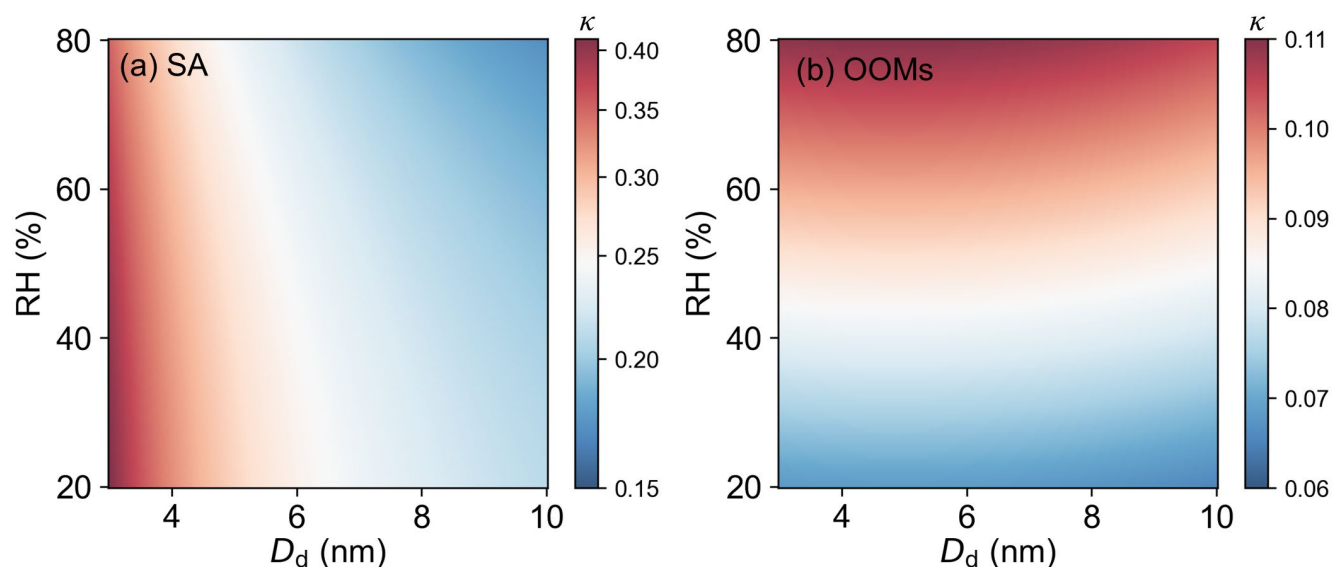
The results of pure inorganic groups and organic groups were shown in Figure 2. The hygroscopicity of 3-10 nm SA particles formed by the oxidation products of SO<sub>2</sub> have significant size dependence.  $\kappa$  values would decrease with  $D_a$ , from  $0.413 \pm 0.011$  for 3 nm to  $0.209 \pm 0.004$  for 10 nm under RH = 20%. It should be noted that the quartz tube was replaced for every single experiment group to eliminate the potential contamination between experiments. Moreover, prior to the hygroscopicity measurements, the oxidation products of SO<sub>2</sub> were characterized using an iodide chemical ionization mass spectrometry (Vocus AIM), which detected no significant organic compound signals in the gas phase (Figure S2). Therefore,

170 this decreasing trend cannot be attributed to organic contamination. Considering the sulfuric acid and water binary nucleation is the basic mechanism for the SA particle formation, the water molecules plays a significant role through hydration (Kulmala et al., 1998; Lee et al., 2019; Stolzenburg et al., 2023; Yu et al., 2017). The initial formation of  $\text{H}_2\text{SO}_4 \cdot \text{H}_2\text{O}$  molecular clusters is followed by rapid addition of further  $\text{H}_2\text{O}$  molecules and these stepwise hydrates process ultimately leads to particles covered with water during growth (Couling et al., 2003; Matsubara et al., 2009). The measured particles were thought as  $(\text{H}_2\text{SO}_4)_m \cdot (\text{H}_2\text{O})_n$  rather than pure  $\text{H}_2\text{SO}_4$ . Consequently, the decreasing trend of  $\kappa$  with particle size may be explained by the increasing water content, which lowers the particles' water uptake capacity relative to their dry mass.

175 Hygroscopicity of SA particles also revealed a consistent decrease with rising RH: at RH = 80%,  $\kappa$  values declined to  $0.361 \pm 0.013$  for 3 nm and  $0.171 \pm 0.011$  for 10 nm particles, decreasing 13% and 18% compared to RH = 20%. This demonstrates that SA particles exhibit reduced hygroscopicity under higher humidity conditions. Although bases such as ammonia/amine could in principle suppress the hygroscopicity of SA particles (Yishake et al., 2025), the  $\kappa$  of an SA-ammonia/amine mixture would be expected to increase with RH, because a higher SA fraction (more acidic) is expected at  
180 higher RH (Chen et al., 2018). This  $\kappa$ -RH dependence is opposite to the trend observed in our study. Moreover, there was no identified source of bases in our system, so ammonia contamination can largely be ruled out. Furthermore, previous studies have shown that the average number of water molecules hydrating each  $\text{H}_2\text{SO}_4$  molecule increases with RH (Kurtén et al., 2007; Temelso et al., 2012; Zollner et al., 2012). Therefore, the observed decrease in hygroscopicity can be attributed to the particles already containing more water at higher RH, resulting in a reduced capacity for additional water uptake.

185 The  $\kappa$  values reported in previous studies are summarized in Table 1. The measured hygroscopicity results in this work are much lower than those reported in previous studies (0.68-0.9, Petters and Kreidenweis, 2007; Shantz et al., 2008; Sullivan et al., 2010), which predicted by thermodynamic model in 30-80 nm based on the model parameters provided by Clegg et al. (1998). The hygroscopicity of newly formed sulfuric acid nanoparticles in CLOUD chamber was examined by a nano hygroscopicity tandem differential mobility analyser (nano-HTDMA) and the reported  $\kappa$  values were  $0.64 \pm 0.02$  and  $0.52 \pm$   
190  $0.02$  for 10 nm and 15 nm, respectively (Kim et al., 2016). The reported variation trend in particle size aligns with our findings but the  $\kappa$  values were much larger than that in this work. While both Kim et al. (2016) and our study report  $\kappa$  values of the oxidation products of  $\text{SO}_2$ , the measurement methods used are fundamentally different. Kim et al. (2016) employed a nano-HTDMA, which measures hygroscopic growth under subsaturated conditions. In contrast, our SFCPC method derives  $\kappa$  values by activating particles under supersaturated conditions. As discussed in previous studies, the measurement condition can  
195 induce inherently different  $\kappa$  values (Biskos et al., 2009; Massling et al., 2023). Specifically, SA particles are expected to exhibit comparably higher hygroscopic growth under subsaturated conditions and lower CCN activity at supersaturation. Therefore, this methodological difference is likely the primary factor contributing to this discrepancy in  $\kappa$  values. In addition, for sub-10 nm particles, the enhanced Kelvin effect (compared to that for larger CCN-size particles) dramatically raises the energy barrier for vapor condensation, directly contributing to suppressed hygroscopicity. Furthermore, the potential size-  
200 dependent influence on phase state may reflect a tendency for nanoparticles to remain in a liquid or mixed phase (Cheng et al., 2015). These nano-size effects on the thermodynamic and physical properties of aerosol particles are likely significant

contributing factors in explaining the distinctively lower  $\kappa$  values observed in our study. As far as we know, direct measurements of the  $\kappa$  of sulfuric acid particles remain limited in the literature, and our results is the first measurement under supersaturation condition in 3-10 nm range.



205

**Figure 2. Dependence of hygroscopicity on particle size and RH: (a) SA formed from  $\text{SO}_2$ , and (b) OOMs from  $\alpha$ -pinene oxidation. Color scale represents the  $\kappa$  values derived from  $f_{\text{org}}$  measurements using SFCPC and EM, where the values were fitted from measurement data to illustrate  $\kappa$  variation trend more clearly.**

Different from the SA results, the OOMs particles formed by the oxidation products of  $\alpha$ -pinene have almost constant  $\kappa$  values in the 3-10 nm diameter range. As shown in Figure 2(b),  $\kappa$  of the pure organic group under 20% RH is  $\sim 0.065$ . This result indicates that the OOMs particles exhibit non-hygroscopicity compared to SA particles and its hygroscopicity has no significant dependence on particle diameter. While the detailed chemical composition of OOMs in these nanoparticles may vary with size due to volatility-dependent partitioning and the Kelvin effect, the observed constancy in  $\kappa$  suggests that the effective hygroscopic properties of the condensing mixture do not change significantly within this size range. This finding is consistent with Frosch et al. (2011), who also observed almost constant  $\kappa$  values ( $0.11 \pm 0.02$ ) for 50-150 nm particles from  $\alpha$ -pinene oxidation. However, to our knowledge, research on particle size dependence is very rare, and no studies have specifically examined the hygroscopicity of  $\alpha$ -pinene oxidation particles in the 3-10 nm size range. Alfarra et al. (2013) measured the hygroscopicity of particles formed from  $\alpha$ -pinene oxidation via both OH radicals and  $\text{O}_3$  using CCNC. Our results align closely with their reported  $\kappa$  values (0.1-0.16), which were also observed under supersaturation conditions. Furthermore, numerous studies have investigated the hygroscopicity of  $\alpha$ -pinene oxidation products using CCNC or HTDMA, reporting a wide range of  $\kappa$  values (0.03-0.19, Cain et al., 2021; Duplissy et al., 2011; Engelhart et al., 2008; Massoli et al., 2010; Razafindrambinina et al., 2022; Wang et al., 2019; Zhao et al., 2016). All experimental results reported here fall within the established range of values found in existing publications.

220

Contrasting with the negligible size dependence, the measured  $\kappa$  values of OOMs exhibited a pronounced increase with RH, rising by 57% from 20% to 80% RH. This finding aligns with Razafindrambinina et al. (2022), who reported higher  $\kappa$  values for laboratory-generated  $\alpha$ -pinene oxidation products under humid conditions ( $\kappa = 0.191$  at 75-80% RH) compared to dry conditions ( $\kappa = 0.130$  at RH < 10%). Similarly, Luo et al. (2024) observed that the molecular composition of  $\alpha$ -pinene oxidation products evolves with increasing RH. While direct molecular-level speciation from our measurements is unavailable, previous studies on  $\alpha$ -pinene oxidation systems provide an explanatory framework. The work of Yuan et al. (2017) suggests that in the presence of water vapor, particles formation may promote the generation of more stable Criegee intermediates, leading to the production of more hygroscopic materials in monoterpene systems. This is supported by evidence of increased formation of oxygenated functional groups, such as multifunctional carboxylic acids, under humid conditions (Poulain et al., 2010). The hygroscopicity of such compounds is intrinsically higher, as the  $\kappa$  increases with the functionality in the following order: ( $-\text{CH}_3$  or  $-\text{NH}_2$ ) < ( $-\text{OH}$ ) < ( $-\text{COOH}$  or  $\text{C}=\text{C}$  or  $\text{C}=\text{O}$ ) (Han et al., 2022). Consequently, the observed increase in  $\kappa$  values at higher RH in this study is attributed to the likely formation of more hygroscopic components.

**Table 1. Summary of  $\kappa$  values of SA and oxidation products of  $\alpha$ -pinene reported in previous studies and this work.**

	$\kappa$ values	Method	$D_a$ (nm)	RH	Reference
	0.9	model	-	-	Petters and Kreidenweis (2007)
	0.68-0.74	model	30-80	-	Shantz et al. (2008)
	0.7	model	-	-	Sullivan et al. (2010)
	$0.64 \pm 0.02$	HTDMA	10	38%	Kim et al. (2016)
	$0.52 \pm 0.02$		15		
SA	$0.413 \pm 0.011$	SFCPC	3	20%	This work
	$0.209 \pm 0.004$		10		
	$0.400 \pm 0.019$		3	40%	
	$0.199 \pm 0.008$		10		
	$0.379 \pm 0.017$		3	60%	
	$0.194 \pm 0.004$		10		
	$0.361 \pm 0.013$		3	80%	
	$0.171 \pm 0.011$		10		
OOMs	0.1-0.16	CCNC	20-500	51.4%-71.4%	Alfarra et al. (2013)
	0.04-0.12	HTDMA	-		
	0.11	CCNC	-	-	Cain et al. (2021)
	0.11-0.19	CCNC	10-450	60%-70%	Zhao et al. (2016)
	0.03-0.06	HTDMA	-		
	$0.130 \pm 0.019$	CCNC	8-352	<10%	Razafindrambinina et al. (2022)
	$0.059 \pm 0.019$	HTDMA	200, 250, 300		
	$0.191 \pm 0.013$	CCNC	8-352	61%	
	$0.042 \pm 0.013$	HTDMA	200, 250, 300		
	$0.065 \pm 0.004$	SFCPC	3	20%	This work

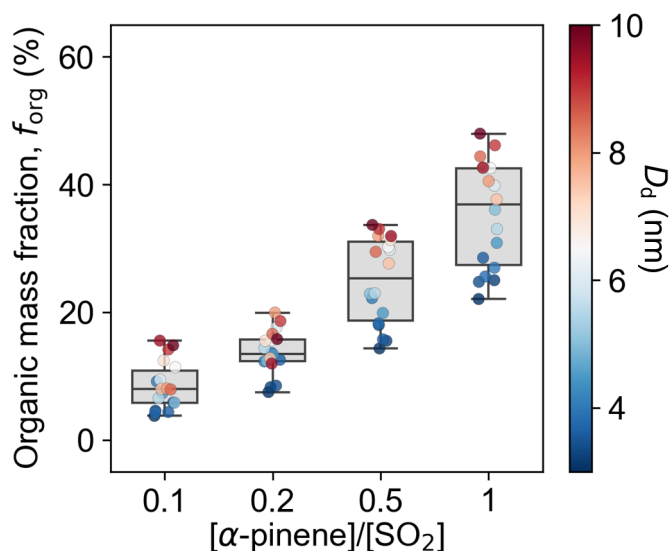
---

	0.066 ± 0.010	10	
	0.076 ± 0.007	3	
	0.076 ± 0.002	10	40%
	0.100 ± 0.006	3	
	0.101 ± 0.009	10	60%
	0.104 ± 0.006	3	
	0.102 ± 0.002	10	80%

---

### 3.2 Organic mass fraction

The  $f_{\text{org}}$  values of 3-10 nm particles was determined using the  $\kappa$ - $f_{\text{org}}$  linear relationship as described in Section 2.3. Figure 240 3 presents the retrieved  $f_{\text{org}}$  results for four experimental groups with varying  $[\alpha\text{-pinene}]/[\text{SO}_2]$  ratios under 20% RH. For 3-10 nm SA-OOMs mixed particles, the median mass fraction of OOMs increased from 7.9% to 36.9% as the  $[\alpha\text{-pinene}]/[\text{SO}_2]$  ratio increased from 0.1 to 1. Considering that ozone was always excessive in the flow tube reactor, the oxidation products of  $\alpha$ -pinene are expected to increase with rising precursor concentration. Consequently, the organic content in the particle phase should be proportional to the concentration of condensable OOMs in the gas phase. This significant increasing trend has also 245 been reported in previous studies. Li et al. (2022) observed that the ratio of particulate organics to sulphate in urban field measurements was positively correlated with the ratio of gaseous condensable organic oxidation products to sulfuric acid. Comprehensive modelling study demonstrated that terpene-rich air masses containing abundant low volatility oxidation products substantially enhanced the condensational growth of nano-particles and dominated the initial growth stage in sub-10 nm, with contribution as high as 95% (Huang et al., 2016). Our experimental results align with these findings, demonstrating 250 that increased organic precursor concentrations significantly elevates the contribution of OOMs to the growth of 3-10 nm particles.

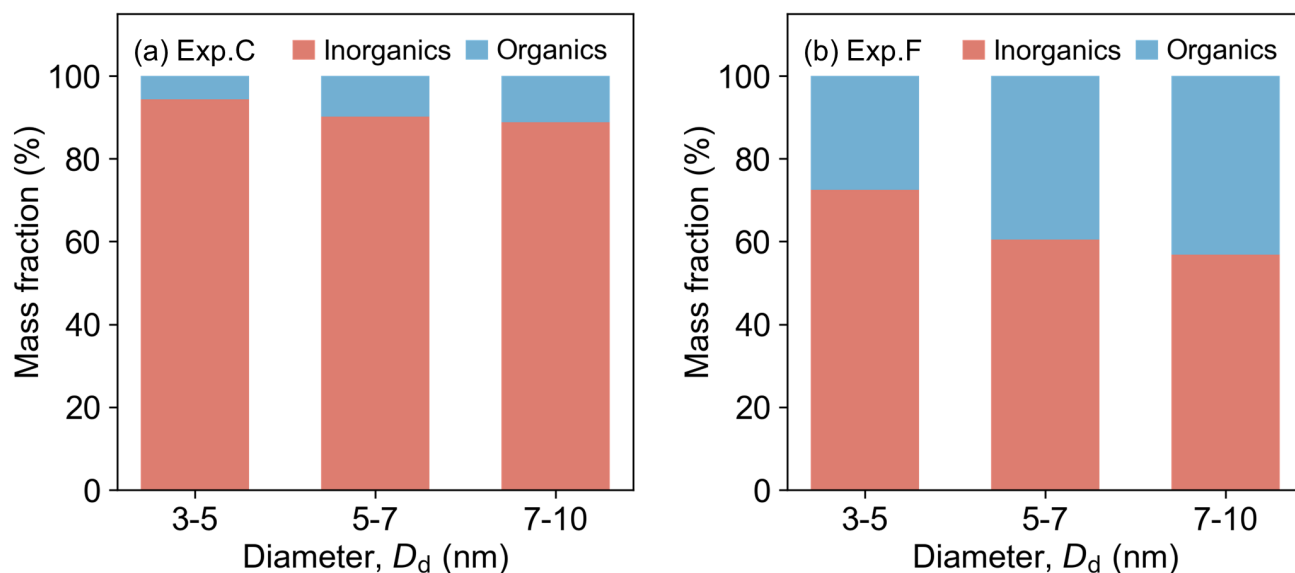


255 **Figure 3. Organic mass fraction as a function of the precursor concentration ratio for SA-OOMs mixture particles at RH 20%. The box plots display the interquartile range (IQR), with the central line denoting the median and whiskers extending to 1.5×IQR. The coloured scatter points represent the mean  $f_{org}$  values for each selected  $D_d$ , as indicated by the colour scale.**

At the same time, our results reveal that the organic content of large particles is generally higher than that of smaller particles (coloured scatter points in Figure 3). To further investigate the size-dependent effect on the chemical composition of nano-particles, the experimental data were analysed by categorizing particles into three distinct size ranges (3-5 nm, 5-7 nm, and 7-10 nm). Figure 4 shows the results from Exp. C and Exp. F, which had the lowest and highest  $[\alpha\text{-pinene}]/[\text{SO}_2]$  ratios of 260 0.1 and 1, respectively. The  $f_{org}$  values for 3-5 nm, 5-7 nm, and 7-10 nm SA-OOMs particles in Exp. C are 5.7%, 9.8% and 11.3%, respectively. Similarly, particles formed in Exp. F contained 27.5%, 39.5%, and 43.2% organics, respectively. These results indicate that the  $f_{org}$  exhibited a consistent increase with  $D_d$  across the range of the precursors mixing ratios examined in this work. Furthermore, these findings demonstrate that  $\alpha$ -pinene oxidation products contributed progressively more to particulate phase in the SA-OOMs system as particle size increased.

265 Several studies have also investigated the chemical composition of newly formed particles in the initial growth stage. Kim et al. (2016) employed nano-HTDMA measurements in the CLOUD chamber to determine  $\kappa$  values, from which volume fractions were derived through linear relationships. Their work revealed that the volume fraction of dimethylamine sulphate in sulfuric acid-dimethylamine systems increased substantially from 0.20-0.29 for 10 nm particles to 0.58-0.92 at 15 nm. Similarly, Keskinen et al. (2013) observed a progressive enhancement in organic volume fraction from 0.4 at 2 nm to 0.9 at 270 63 nm, while noting the existing measurement challenges for particles between 2-15 nm where chemical characterization remains particularly difficult. More recently, Li et al. (2022) achieved direct measurements of size-resolved molecular composition using TDCIMS, demonstrating a clear increase in organic mass fraction with particle diameter across the 8-40 nm range in urban Beijing. Other studies have also indicated that particle growth mechanisms exhibit a dependence on particle size (Riipinen et al., 2012). The contribution of SA decreased as particle size increased (Xiao et al., 2015), while organic

275 compounds increasingly dominated the growth process, showing a strong size-dependent effect (Riccobono et al., 2012). Our experimental results align well with these previous studies, confirming that organic contributions to nanoparticle growth exhibit consistent size dependence, while additionally providing novel composition data for freshly nucleated particles as small as 3 nm, thereby extending the current understanding of early particle growth.



280 **Figure 4. Organic mass fraction of SA-OOMs mixtures as a function of particles diameter range with two precursors mixing ratios: (a) 0.1 for Exp. C, (b) 1 for Exp. F. Red and blue bars represent  $f_{\text{org}}$  values of inorganics (SA) and organics (OOMs). Note that the size ranges are defined as semi-open intervals, except for the first bin which includes its lower bound.**

### 3.3 Effect of relative humidity

To investigate the effect of humidity on the initial growth of newly formed particles, we increased RH from 20% to 80% and measured the organic content across this range. The retrieved  $f_{\text{org}}$  values were similarly grouped by particle size, following the same methodology as in the size-dependence analysis. The results from all RH experimental groups (20%-80%) were compared with those under 20% RH to examine the relative change in organic contribution with increasing RH (Figure 5). The enhancement of organic contribution to particle growth by humidity exhibits a marked difference between particles below and above 5 nm. Taking Exp. D as an example, the  $f_{\text{org}}$  for 3-5 nm particles began to increase from 60% RH, with a relative increment reaching approximately 47% at 80% RH. For particles in the 5-7 nm and 7-10 nm size ranges,  $f_{\text{org}}$  exhibited a sharp increase starting at 40% RH and remained almost stable within the 40%-80% RH range. Compared to the condition at 20% RH, the organic contribution to particle growth was enhanced by about 52% and 81%, respectively. We speculate that these behaviours arise from the competing influences of humidity on the physicochemical properties of  $\alpha$ -pinene oxidation products and the Kelvin effect. For such small nanoparticles, the partitioning of a molecule into the particulate phase is influenced by both its volatility and the Kelvin effect (Riipinen et al., 2012). Previous molecular measurements in both gas and particle phases have reported increased yields at elevated RH (Poulain et al., 2010). Concurrently, Surdu et al. (2023) observed that  $\alpha$ -

pinene oxidation products become more volatile under humid conditions. The relative stability of  $f_{\text{org}}$  in the 3-5 nm particles at low RH condition may thus be explained by a balance between these two competing mechanisms, where the heightened Kelvin effect presents a significant barrier to condensation. For larger particles, the diminished Kelvin effect facilitates the condensation of organic compounds, allowing even more volatile products to contribute to nanoparticle growth. The distinct response patterns, where the enhancement occurred gradually for 3-5 nm particles but sharply for larger particles, suggest that the Kelvin effect plays a more dominant role for the smallest particle growth at lower RH. Overall, increased RH enhances the organic contribution by altering the properties of  $\alpha$ -pinene oxidation products, with a more pronounced effect observed for larger particles.

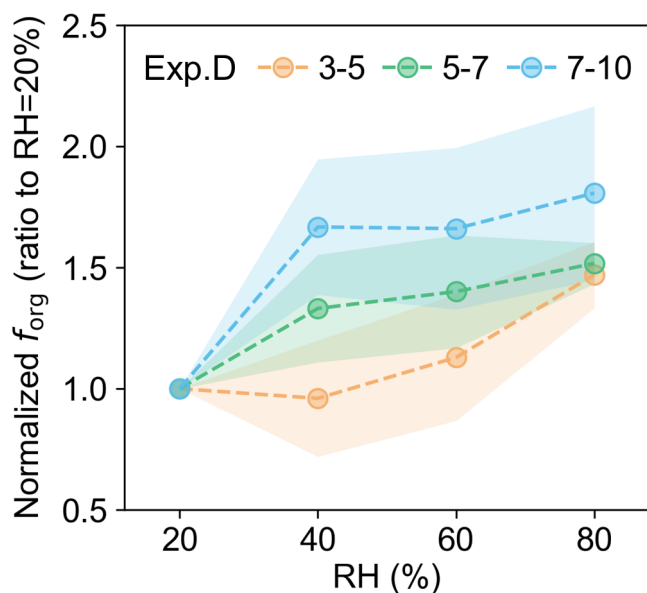


Figure 5. Relative change in  $f_{\text{org}}$  for 3-5 nm, 5-7 nm, and 7-10 nm particles as a function of RH. Data points indicate  $f_{\text{org}}$  values normalized to measurements at 20% RH. Shaded areas represent the standard deviation for each size range.

#### 4 Conclusion

In this study, a flow tube reactor was employed to conduct a series of experiments investigating nucleation and particle growth across a wide range of RH (20%-80%).  $\text{SO}_2$  and  $\alpha$ -pinene served as gas-phase precursors for the formation of SA and OOMs in all experiments, with the precursor concentration ratio  $[\alpha\text{-pinene}]/[\text{SO}_2]$  varying from 0.1 to 1. A custom-designed SFCPC was utilized to quantify the size-resolved hygroscopicity. Based on the linear relationship between  $\kappa$  and  $f_{\text{org}}$ , the organic mass fraction of freshly formed particles was determined within the 3-10 nm diameter range.

Our work provides quantitative insight into the distinct hygroscopic behaviours of SA and OOMs. For SA,  $\kappa$  exhibited significant size dependence, decreasing from  $0.413 \pm 0.011$  at 3 nm to  $0.209 \pm 0.004$  at 10 nm under 20% RH. When RH was elevated to 80%,  $\kappa$  further declined by 18% (to  $0.171 \pm 0.011$  at 10 nm). This decrease may be explained by the formation of

(H<sub>2</sub>SO<sub>4</sub>)<sub>m</sub>-(H<sub>2</sub>O)<sub>n</sub> complexes. The hydration process eventually results in water-covered particles, reducing their capacity for further water uptake. The measured  $\kappa$  values in this work are much lower than those reported in previous studies and this discrepancy may be attributed to the nano size effect and different measurement techniques. In contrast,  $\kappa$  of OOMs remained relatively constant across the 3-10 nm size range but increased with rising RH (from  $0.069 \pm 0.003$  to  $0.108 \pm 0.004$  as RH rose from 20% to 80%) potentially involving changes in the physicochemical properties of the oxidation products. These experimental findings are consistent with previously reported  $\kappa$  values for  $\alpha$ -pinene oxidation particles, which typically range from 0.03 to 0.19. The derived organic content of SA-OOMs mixed particles consistently increased with higher [ $\alpha$ -pinene]/[SO<sub>2</sub>] ratios, indicating enhanced contribution of organics to the particulate phase. Furthermore,  $f_{\text{org}}$  exhibited a consistent increase with particle size. Specifically,  $f_{\text{org}}$  values increased from 5.67% to 11.25% and from 27.47% to 43.22% for [ $\alpha$ -pinene]/[SO<sub>2</sub>] of 0.1 and 1, respectively. This demonstrated that the contribution of  $\alpha$ -pinene oxidation products to particulate phase in the SA-OOMs system became more pronounced at larger particles. Our results align with previous studies, further confirming the size dependence of organic contributions to nanoparticle growth and additionally providing novel composition data down to 3 nm. The effects of RH on chemical composition revealed distinct trends in  $f_{\text{org}}$  across different size ranges: for 3-5 nm particles,  $f_{\text{org}}$  varied negligibly until 60% RH, while for 5-10 nm particles, it increased with RH and had nearly stabilized at 40% RH. These observations may be associated with a combination of factors including the Kelvin effect as well as increased volatility and higher yields under elevated RH.

To the best of our knowledge, this is the first study to measure the hygroscopicity ( $\kappa$ ) of particles composed of SA and  $\alpha$ -pinene-derived OOMs down to 3 nm. Given that direct measurements of chemical composition for newly formed 3-10 nm particles remain limited in the literature, our study provides important, quantitative, and size-resolved organic content data in this nano size range. The experimental results of SA-OOMs mixture indicate that OOMs contribute significantly to the particulate phase, with their mass fraction increasing with particle size, [ $\alpha$ -pinene]/[SO<sub>2</sub>] ratio, and RH. These findings provide valuable supplementary information for advancing our understanding of new particle formation and subsequent growth. Looking ahead, exploring of multi-precursor systems, longer oxidation times for better simulating aging processes, and the further deployment of the SFCPC in field measurements will yield deeper insights into the chemical composition of atmospheric aerosols.

**Author contributions:** KZ and ZW contributed to the methodology, data curation, and writing of the original draft. ZX and FZ contributed to the reviewing and editing. ZW contributed to the supervision, funding acquisition, conceptualization, investigation, data curation, writing, reviewing, and editing.

345 **Competing interests:** At least one of the (co-)authors is a member of the editorial board of Atmospheric Chemistry and Physics.

**Data availability:** Data are available upon request to the corresponding author.

**Acknowledgements:** This study was supported by the National Natural Science Foundation of China (41805100, 91844301, 42005086) and the National Key Research and Development Program of China (2022YFC3703505).

350 **References**

- Alfarra, M. R., Good, N., Wyche, K. P., Hamilton, J. F., Monks, P. S., Lewis, A. C., and McFiggans, G.: Water uptake is independent of the inferred composition of secondary aerosols derived from multiple biogenic VOCs, *Atmos. Chem. Phys.*, 13, 11769–11789, <https://doi.org/10.5194/acp-13-11769-2013>, 2013.
- 355 Berndt, T., Böge, O., Stratmann, F., Heintzenberg, J., and Kulmala, M.: Rapid formation of sulfuric acid particles at near-atmospheric conditions, *Science*, 307, 698–700, <https://doi.org/10.1126/science.1104054>, 2005.
- Berndt, T., Richters, S., Jokinen, T., Hyttinen, N., Kurtén, T., Otkjær, R. V., Kjaergaard, H. G., Stratmann, F., Herrmann, H., Sipilä, M., Kulmala, M., and Ehn, M.: Hydroxyl radical-induced formation of highly oxidized organic compounds, *Nat Commun*, 7, 13677, <https://doi.org/10.1038/ncomms13677>, 2016.
- 360 Bianchi, F., Kurtén, T., Riva, M., Mohr, C., Rissanen, M. P., Roldin, P., Berndt, T., Crouse, J. D., Wennberg, P. O., Mentel, T. F., Wildt, J., Junninen, H., Jokinen, T., Kulmala, M., Worsnop, D. R., Thornton, J. A., Donahue, N., Kjaergaard, H. G., and Ehn, M.: Highly oxygenated organic molecules (HOM) from gas-phase autoxidation involving peroxy radicals: A key contributor to atmospheric aerosol, *Chem. Rev.*, 119, 3472–3509, <https://doi.org/10.1021/acs.chemrev.8b00395>, 2019.
- Biskos, G., Buseck, P. R., and Martin, S. T.: Hygroscopic growth of nucleation-mode acidic sulfate particles, *J. Aerosol Sci.*, 40, 338–347, <https://doi.org/10.1016/j.jaerosci.2008.12.003>, 2009.
- 365 Cain, K. P., Liangou, A., Davidson, M. L., and Pandis, S. N.:  $\alpha$ -pinene, limonene, and cyclohexene secondary organic aerosol hygroscopicity and oxidation level as a function of volatility, *Aerosol Air Qual. Res.*, 21, 200511, <https://doi.org/10.4209/aaqr.2020.08.0511>, 2021.
- Chen, H., Chee, S., Lawler, M. J., Barsanti, K. C., Wong, B. M., and Smith, J. N.: Size resolved chemical composition of nanoparticles from reactions of sulfuric acid with ammonia and dimethylamine, *Aerosol Sci. Technol.*, 52, 1120–1133, <https://doi.org/10.1080/02786826.2018.1490005>, 2018.
- 370 Cheng, Y., Su, H., Koop, T., Mikhailov, E., and Pöschl, U.: Size dependence of phase transitions in aerosol nanoparticles, *Nat. Commun.*, 6, 5923, <https://doi.org/10.1038/ncomms6923>, 2015.
- Clegg, S. L., Brimblecombe, P., and Wexler, A. S.: Thermodynamic Model of the System  $\text{H}^+ - \text{NH}_4^+ - \text{Na}^+ - \text{SO}_4^{2-} - \text{NO}_3^- - \text{Cl}^- - \text{H}_2\text{O}$  at 298.15 K, *J. Phys. Chem. A*, 102, 2155–2171, <https://doi.org/10.1021/jp973043j>, 1998.
- 375 Couling, S. B., Fletcher, J., Horn, A. B., Newnham, D. A., McPheat, R. A., and Gary Williams, R.: First detection of molecular hydrate complexes in sulfuric acid aerosols, *Phys. Chem. Chem. Phys.*, 5, 4108, <https://doi.org/10.1039/B306620G>, 2003.
- Du, W., Zhao, J., Dada, L., Xu, W., Wang, Y., Shi, Y., Chen, X., Kokkonen, T. V., Cai, J., Zhang, Y., Wang, Q., Cai, R., Zha, Q., Zhou, L., Li, Z., Yu, F., Fu, P., Hu, F., Wang, Z., Worsnop, D. R., Bianchi, F., Kerminen, V.-M., Kulmala, M., and Sun, Y.: Impacts of enhanced new-particle growth events above urban roughness sublayer on cloud condensation nuclei, *One Earth*, 101169, <https://doi.org/10.1016/j.oneear.2024.12.005>, 2024.
- 385 Dunne, E. M., Gordon, H., Kürten, A., Almeida, J., Duplissy, J., Williamson, C., Ortega, I. K., Pringle, K. J., Adamov, A., Baltensperger, U., Barmet, P., Benduhn, F., Bianchi, F., Breitenlechner, M., Clarke, A., Curtius, J., Dommen, J., Donahue, N. M., Ehrhart, S., Flagan, R. C., Franchin, A., Guida, R., Hakala, J., Hansel, A., Heinritzi, M., Jokinen, T., Kangasluoma, J., Kirkby, J., Kulmala, M., Kupc, A., Lawler, M. J., Lehtipalo, K., Makhmutov, V., Mann, G., Mathot, S., Merikanto, J., Miettinen, P., Nenes, A., Onnela, A., Rap, A., Reddington, C. L. S., Riccobono, F., Richards, N. A. D., Rissanen, M. P., Rondo, L., Sarnela, N., Schobesberger, S., Sengupta, K., Simon, M., Sipilä, M., Smith, J. N., Stozhkov, Y., Tomé, A., Tröstl, J.,

- Wagner, P. E., Wimmer, D., Winkler, P. M., Worsnop, D. R., and Carslaw, K. S.: Global atmospheric particle formation from CERN CLOUD measurements, *Science*, 354, 1119–1124, <https://doi.org/10.1126/science.aaf2649>, 2016.
- 390 Duplissy, J., DeCarlo, P. F., Dommen, J., Alfarra, M. R., Metzger, A., Barmapadimos, I., Prevot, A. S. H., Weingartner, E., Tritscher, T., Gysel, M., Aiken, A. C., Jimenez, J. L., Canagaratna, M. R., Worsnop, D. R., Collins, D. R., Tomlinson, J., and Baltensperger, U.: Relating hygroscopicity and composition of organic aerosol particulate matter, *Atmos. Chem. Phys.*, 11, 1155–1165, <https://doi.org/10.5194/acp-11-1155-2011>, 2011.
- 395 Dusek, U., Frank, G. P., Curtius, J., Drewnick, F., Schneider, J., Kürten, A., Rose, D., Andreae, M. O., Borrmann, S., and Pöschl, U.: Enhanced organic mass fraction and decreased hygroscopicity of cloud condensation nuclei (CCN) during new particle formation events, *Geophys. Res. Lett.*, 37, 2009GL040930, <https://doi.org/10.1029/2009GL040930>, 2010.
- 400 Ehn, M., Thornton, J. A., Kleist, E., Sipilä, M., Junninen, H., Pullinen, I., Springer, M., Rubach, F., Tillmann, R., Lee, B., Lopez-Hilfiker, F., Andres, S., Acir, I.-H., Rissanen, M., Jokinen, T., Schobesberger, S., Kangasluoma, J., Kontkanen, J., Nieminen, T., Kurtén, T., Nielsen, L. B., Jørgensen, S., Kjaergaard, H. G., Canagaratna, M., Maso, M. D., Berndt, T., Petäjä, T., Wahner, A., Kerminen, V.-M., Kulmala, M., Worsnop, D. R., Wildt, J., and Mentel, T. F.: A large source of low-volatility secondary organic aerosol, *Nature*, 506, 476–479, <https://doi.org/10.1038/nature13032>, 2014.
- Engelhart, G. J., Asa-Awuku, A., Nenes, A., and Pandis, S. N.: CCN activity and droplet growth kinetics of fresh and aged monoterpene secondary organic aerosol, *Atmos. Chem. Phys.*, 8, 3937–3949, <https://doi.org/10.5194/acp-8-3937-2008>, 2008.
- Frosch, M., Bilde, M., DeCarlo, P. F., Jurányi, Z., Tritscher, T., Dommen, J., Donahue, N. M., Gysel, M., Weingartner, E., and Baltensperger, U.: Relating cloud condensation nuclei activity and oxidation level of  $\alpha$ -pinene secondary organic aerosols: CCN AND OXIDATION LEVEL OF  $\alpha$ -PINENE SOA, *J. Geophys. Res.*, 116, n/a-n/a, <https://doi.org/10.1029/2011JD016401>, 2011.
- Fuchs, N. A.: On the stationary charge distribution on aerosol particles in a bipolar ionic atmosphere, *Geofis. Pura Appl.*, 56, 185–193, <https://doi.org/10.1007/BF01993343>, 1963.
- 410 Han, S., Hong, J., Luo, Q., Xu, H., Tan, H., Wang, Q., Tao, J., Zhou, Y., Peng, L., He, Y., Shi, J., Ma, N., Cheng, Y., and Su, H.: Hygroscopicity of organic compounds as a function of organic functionality, water solubility, molecular weight, and oxidation level, *Atmos. Chem. Phys.*, 22, 3985–4004, <https://doi.org/10.5194/acp-22-3985-2022>, 2022.
- Huang, X., Zhou, L., Ding, A., Qi, X., Nie, W., Wang, M., Chi, X., Petäjä, T., Kerminen, V.-M., Roldin, P., Rusanen, A., Kulmala, M., and Boy, M.: Comprehensive modelling study on observed new particle formation at the SORPES station in nanjing, China, *Atmos. Chem. Phys.*, 16, 2477–2492, <https://doi.org/10.5194/acp-16-2477-2016>, 2016.
- 415 Iyer, S., Rissanen, M. P., Valiev, R., Barua, S., Krechmer, J. E., Thornton, J., Ehn, M., and Kurtén, T.: Molecular mechanism for rapid autoxidation in  $\alpha$ -pinene ozonolysis, *Nat Commun*, 12, 878, <https://doi.org/10.1038/s41467-021-21172-w>, 2021.
- Jayne, J. T., Pöschl, U., Chen, Y., Dai, D., Molina, L. T., Worsnop, D. R., Kolb, C. E., and Molina, M. J.: Pressure and temperature dependence of the gas-phase reaction of SO<sub>3</sub> with H<sub>2</sub>O and the heterogeneous reaction of SO<sub>3</sub> with H<sub>2</sub>O/H<sub>2</sub>SO<sub>4</sub> surfaces, *J. Phys. Chem. A*, 101, 10000–10011, <https://doi.org/10.1021/jp972549z>, 1997.
- 420 Jimenez, J. L., Canagaratna, M. R., Donahue, N. M., Prevot, A. S. H., Zhang, Q., Kroll, J. H., DeCarlo, P. F., Allan, J. D., Coe, H., Ng, N. L., Aiken, A. C., Docherty, K. S., Ulbrich, I. M., Grieshop, A. P., Robinson, A. L., Duplissy, J., Smith, J. D., Wilson, K. R., Lanz, V. A., Hueglin, C., Sun, Y. L., Tian, J., Laaksonen, A., Raatikainen, T., Rautiainen, J., Vaattovaara, P., Ehn, M., Kulmala, M., Tomlinson, J. M., Collins, D. R., Cubison, M. J., E., Dunlea, J., Huffman, J. A., Onasch, T. B., Alfarra, M. R., Williams, P. I., Bower, K., Kondo, Y., Schneider, J., Drewnick, F., Borrmann, S., Weimer, S., Demerjian, K., Salcedo, D., Cottrell, L., Griffin, R., Takami, A., Miyoshi, T., Hatakeyama, S., Shimono, A., Sun, J. Y., Zhang, Y. M., Dzepina, K., Kimmel,
- 425

- J. R., Sueper, D., Jayne, J. T., Herndon, S. C., Trimborn, A. M., Williams, L. R., Wood, E. C., Middlebrook, A. M., Kolb, C. E., Baltensperger, U., and Worsnop, D. R.: Evolution of organic aerosols in the atmosphere, *Science*, 326, 1525–1529, <https://doi.org/10.1126/science.1180353>, 2009.
- 430 Kang, S., Wildt, J., Pullinen, I., Vereecken, L., Wu, C., Wahner, A., Zorn, S. R., and Mentel, T. F.: Formation of highly oxygenated organic molecules from  $\alpha$ -pinene photooxidation: Evidence for the importance of highly oxygenated alkoxy radicals, *Atmos. Chem. Phys.*, 25, 15715–15740, <https://doi.org/10.5194/acp-25-15715-2025>, 2025.
- Kangasluoma, J., Kuang, C., Wimmer, D., Rissanen, M. P., Lehtipalo, K., Ehn, M., Worsnop, D. R., Wang, J., Kulmala, M., and Petäjä, T.: Sub-3 nm particle size and composition dependent response of a nano-CPC battery, *Atmos. Meas. Tech.*, 7, 689–700, <https://doi.org/10.5194/amt-7-689-2014>, 2014.
- 435 Keskinen, H., Virtanen, A., Joutsensaari, J., Tsagkogeorgas, G., Duplissy, J., Schobesberger, S., Gysel, M., Riccobono, F., Slowik, J. G., Bianchi, F., Yli-Juuti, T., Lehtipalo, K., Rondo, L., Breitenlechner, M., Kupc, A., Almeida, J., Amorim, A., Dunne, E. M., Downard, A. J., Ehrhart, S., Franchin, A., Kajos, M. K., Kirkby, J., Kürten, A., Nieminen, T., Makhmutov, V., Mathot, S., Miettinen, P., Onnela, A., Petäjä, T., Praplan, A., Santos, F. D., Schallhart, S., Sipilä, M., Stozhkov, Y., Tomé, A., Vaattovaara, P., Wimmer, D., Prevot, A., Dommen, J., Donahue, N. M., Flagan, R. C., Weingartner, E., Viisanen, Y., Riipinen, I., Hansel, A., Curtius, J., Kulmala, M., Worsnop, D. R., Baltensperger, U., Wex, H., Stratmann, F., and Laaksonen, A.: Evolution of particle composition in CLOUD nucleation experiments, *Atmos. Chem. Phys.*, 13, 5587–5600, <https://doi.org/10.5194/acp-13-5587-2013>, 2013.
- 445 Kim, J., Ahlm, L., Yli-Juuti, T., Lawler, M., Keskinen, H., Tröstl, J., Schobesberger, S., Duplissy, J., Amorim, A., Bianchi, F., Donahue, N. M., Flagan, R. C., Hakala, J., Heinritzi, M., Jokinen, T., Kürten, A., Laaksonen, A., Lehtipalo, K., Miettinen, P., Petäjä, T., Rissanen, M. P., Rondo, L., Sengupta, K., Simon, M., Tomé, A., Williamson, C., Wimmer, D., Winkler, P. M., Ehrhart, S., Ye, P., Kirkby, J., Curtius, J., Baltensperger, U., Kulmala, M., Lehtinen, K. E. J., Smith, J. N., Riipinen, I., and Virtanen, A.: Hygroscopicity of nanoparticles produced from homogeneous nucleation in the CLOUD experiments, *Atmos. Chem. Phys.*, 16, 293–304, <https://doi.org/10.5194/acp-16-293-2016>, 2016.
- 450 Kirkby, J., Duplissy, J., Sengupta, K., Frege, C., Gordon, H., Williamson, C., Heinritzi, M., Simon, M., Yan, C., Almeida, J., Tröstl, J., Nieminen, T., Ortega, I. K., Wagner, R., Adamov, A., Amorim, A., Bernhammer, A.-K., Bianchi, F., Breitenlechner, M., Brilke, S., Chen, X., Craven, J., Dias, A., Ehrhart, S., Flagan, R. C., Franchin, A., Fuchs, C., Guida, R., Hakala, J., Hoyle, C. R., Jokinen, T., Junninen, H., Kangasluoma, J., Kim, J., Krapf, M., Kürten, A., Laaksonen, A., Lehtipalo, K., Makhmutov, V., Mathot, S., Molteni, U., Onnela, A., Peräkylä, O., Piel, F., Petäjä, T., Praplan, A. P., Pringle, K., Rap, A., Richards, N. A. D., Riipinen, I., Rissanen, M. P., Rondo, L., Sarnela, N., Schobesberger, S., Scott, C. E., Seinfeld, J. H., Sipilä, M., Steiner, G., Stozhkov, Y., Stratmann, F., Tomé, A., Virtanen, A., Vogel, A. L., Wagner, A. C., Wagner, P. E., Weingartner, E., Wimmer, D., Winkler, P. M., Ye, P., Zhang, X., Hansel, A., Dommen, J., Donahue, N. M., Worsnop, D. R., Baltensperger, U., Kulmala, M., Carslaw, K. S., and Curtius, J.: Ion-induced nucleation of pure biogenic particles, *Nature*, 533, 521–526, <https://doi.org/10.1038/nature17953>, 2016.
- 460 Kirkby, J., Amorim, A., Baltensperger, U., Carslaw, K. S., Christoudias, T., Curtius, J., Donahue, N. M., Haddad, I. E., Flagan, R. C., Gordon, H., Hansel, A., Harder, H., Junninen, H., Kulmala, M., Kürten, A., Laaksonen, A., Lehtipalo, K., Lelieveld, J., Möhler, O., Riipinen, I., Stratmann, F., Tomé, A., Virtanen, A., Volkamer, R., Winkler, P. M., and Worsnop, D. R.: Atmospheric new particle formation from the CERN CLOUD experiment, *Nat. Geosci.*, 16, 948–957, <https://doi.org/10.1038/s41561-023-01305-0>, 2023.
- 465 Kuang, C., Riipinen, I., Sihto, S.-L., Kulmala, M., McCormick, A. V., and McMurry, P. H.: An improved criterion for new particle formation in diverse atmospheric environments, *Atmos. Chem. Phys.*, 10, 8469–8480, <https://doi.org/10.5194/acp-10-8469-2010>, 2010.
- Kulmala, M.: How particles nucleate and grow, *Science*, 302, 1000–1001, <https://doi.org/10.1126/science.1090848>, 2003.

- Kulmala, M., Laaksonen, A., and Pirjola, L.: Parameterizations for sulfuric acid/water nucleation rates, *J. Geophys. Res.-Atmos.*, 103, 8301–8307, <https://doi.org/10.1029/97JD03718>, 1998.
- 470 Kulmala, M., Mordas, G., Petäjä, T., Grönholm, T., Aalto, P. P., Vehkamäki, H., Hienola, A. I., Herrmann, E., Sipilä, M., Riipinen, I., Manninen, H. E., Hämeri, K., Stratmann, F., Bilde, M., Winkler, P. M., Birmili, W., and Wagner, P. E.: The condensation particle counter battery (CPCB): A new tool to investigate the activation properties of nanoparticles, *J. Aerosol. Sci.*, 38, 289–304, <https://doi.org/10.1016/j.jaerosci.2006.11.008>, 2007.
- 475 Kulmala, M., Kontkanen, J., Junninen, H., Lehtipalo, K., Manninen, H. E., Nieminen, T., Petäjä, T., Sipilä, M., Schobesberger, S., Rantala, P., Franchin, A., Jokinen, T., Järvinen, E., Äijälä, M., Kangasluoma, J., Hakala, J., Aalto, P. P., Paasonen, P., Mikkilä, J., Vanhanen, J., Aalto, J., Hakola, H., Makkonen, U., Ruuskanen, T., Mauldin, R. L., Duplissy, J., Vehkamäki, H., Bäck, J., Kortelainen, A., Riipinen, I., Kurtén, T., Johnston, M. V., Smith, J. N., Ehn, M., Mentel, T. F., Lehtinen, K. E. J., Laaksonen, A., Kerminen, V.-M., and Worsnop, D. R.: Direct observations of atmospheric aerosol nucleation, *Science*, 339, 943–946, <https://doi.org/10.1126/science.1227385>, 2013.
- 480 Kulmala, M., Petäjä, T., Ehn, M., Thornton, J., Sipilä, M., Worsnop, D. R., and Kerminen, V.-M.: Chemistry of atmospheric nucleation: On the recent advances on precursor characterization and atmospheric cluster composition in connection with atmospheric new particle formation, *Annu. Rev. Phys. Chem.*, 65, 21–37, <https://doi.org/10.1146/annurev-physchem-040412-110014>, 2014.
- 485 Kurtén, T., Noppel, M., Vehkamäki, H., Salonen, M., and Kulmala, M.: Quantum chemical studies of hydrate formation of H<sub>2</sub>SO<sub>4</sub> and HSO<sub>4</sub><sup>-</sup> - ProQuest, Boreal Environ. Res., 2007.
- Lee, S., Gordon, H., Yu, H., Lehtipalo, K., Haley, R., Li, Y., and Zhang, R.: New Particle Formation in the Atmosphere: From Molecular Clusters to Global Climate, *J. Geophys. Res.-Atmos.*, 124, 7098–7146, <https://doi.org/10.1029/2018JD029356>, 2019.
- 490 Li, X., Li, Y., Lawler, M. J., Hao, J., Smith, J. N., and Jiang, J.: Composition of ultrafine particles in urban beijing: Measurement using a thermal desorption chemical ionization mass spectrometer, *Environ. Sci. Technol.*, 55, 2859–2868, <https://doi.org/10.1021/acs.est.0c06053>, 2021.
- 495 Li, X., Li, Y., Cai, R., Yan, C., Qiao, X., Guo, Y., Deng, C., Yin, R., Chen, Y., Li, Y., Yao, L., Sarnela, N., Zhang, Y., Petäjä, T., Bianchi, F., Liu, Y., Kulmala, M., Hao, J., Smith, J. N., and Jiang, J.: Insufficient condensable organic vapors lead to slow growth of new particles in an urban environment, *Environ. Sci. Technol.*, 56, 9936–9946, <https://doi.org/10.1021/acs.est.2c01566>, 2022.
- Lovejoy, E. R., Hanson, D. R., and Huey, L. G.: Kinetics and products of the gas-phase reaction of SO<sub>3</sub> with water, *J. Phys. Chem.*, 100, 19911–19916, <https://doi.org/10.1021/jp962414d>, 1996.
- 500 Luo, H., Guo, Y., Shen, H., Huang, D. D., Zhang, Y., and Zhao, D.: Effect of relative humidity on the molecular composition of secondary organic aerosols from  $\alpha$ -pinene ozonolysis, *Environ. Sci.: Atmos.*, 4, 519–530, <https://doi.org/10.1039/D3EA00149K>, 2024.
- Massling, A., Lange, R., Pernov, J. B., Gosewinkel, U., Sørensen, L.-L., and Skov, H.: Measurement report: High arctic aerosol hygroscopicity at sub- and supersaturated conditions during spring and summer, *Atmos. Chem. Phys.*, 23, 4931–4953, <https://doi.org/10.5194/acp-23-4931-2023>, 2023.
- 505 Massoli, P., Lambe, A. T., Ahern, A. T., Williams, L. R., Ehn, M., Mikkilä, J., Canagaratna, M. R., Brune, W. H., Onasch, T. B., Jayne, J. T., Petäjä, T., Kulmala, M., Laaksonen, A., Kolb, C. E., Davidovits, P., and Worsnop, D. R.: Relationship between

- aerosol oxidation level and hygroscopic properties of laboratory generated secondary organic aerosol (SOA) particles, *Geophys. Res. Lett.*, 37, 2010GL045258, <https://doi.org/10.1029/2010GL045258>, 2010.
- Matsubara, H., Ebisuzaki, T., and Yasuoka, K.: Microscopic insights into nucleation in a sulfuric acid–water vapor mixture based on molecular dynamics simulation, *J. Chem. Phys.*, 130, 104705, <https://doi.org/10.1063/1.3082079>, 2009.
- 510 O’Dowd, C. D., Aalto, P., Hmeri, K., Kulmala, M., and Hoffmann, T.: Atmospheric particles from organic vapours, *Nature*, 416, 497–498, <https://doi.org/10.1038/416497a>, 2002.
- Petters, M. D. and Kreidenweis, S. M.: A single parameter representation of hygroscopic growth and cloud condensation nucleus activity, *Atmos. Chem. Phys.*, 7, 1961–1971, <https://doi.org/10.5194/acp-7-1961-2007>, 2007.
- 515 Pöhlker, M. L., Pöhlker, C., Quaas, J., Mülmenstädt, J., Pozzer, A., Andreae, M. O., Artaxo, P., Block, K., Coe, H., Ervens, B., Gallimore, P., Gaston, C. J., Gunthe, S. S., Henning, S., Herrmann, H., Krüger, O. O., McFiggans, G., Poulain, L., Raj, S. S., Reyes-Villegas, E., Royer, H. M., Walter, D., Wang, Y., and Pöschl, U.: Global organic and inorganic aerosol hygroscopicity and its effect on radiative forcing, *Nat. Commun.*, 14, 6139, <https://doi.org/10.1038/s41467-023-41695-8>, 2023.
- 520 Poulain, L., Wu, Z., Petters, M. D., Wex, H., Hallbauer, E., Wehner, B., Massling, A., Kreidenweis, S. M., and Stratmann, F.: Towards closing the gap between hygroscopic growth and CCN activation for secondary organic aerosols – Part 3: Influence of the chemical composition on the hygroscopic properties and volatile fractions of aerosols, *Atmos. Chem. Phys.*, 10, 3775–3785, <https://doi.org/10.5194/acp-10-3775-2010>, 2010.
- Razafindrabinina, P. N., Malek, K. A., Dawson, J. N., DiMonte, K., Raymond, T. M., Dutcher, D. D., Freedman, M. A., and Asa-Awuku, A.: Hygroscopicity of internally mixed ammonium sulfate and secondary organic aerosol particles formed at low and high relative humidity, *Environ. Sci.: Atmos.*, 2, 202–214, <https://doi.org/10.1039/D1EA00069A>, 2022.
- 525 Ren, J., Chen, L., Fan, T., Liu, J., Jiang, S., and Zhang, F.: The NPF effect on CCN number concentrations: A review and re-evaluation of observations from 35 sites worldwide, *Geophys. Res. Lett.*, 48, e2021GL095190, <https://doi.org/10.1029/2021GL095190>, 2021.
- Riccobono, F., Rondo, L., Sipilä, M., Barmet, P., Curtius, J., Dommen, J., Ehn, M., Ehrhart, S., Kulmala, M., Kürten, A., Mikkilä, J., Paasonen, P., Petäjä, T., Weingartner, E., and Baltensperger, U.: Contribution of sulfuric acid and oxidized organic compounds to particle formation and growth, *Atmos. Chem. Phys.*, 12, 9427–9439, <https://doi.org/10.5194/acp-12-9427-2012>, 2012.
- 530 Riccobono, F., Schobesberger, S., Scott, C. E., Dommen, J., Ortega, I. K., Rondo, L., Almeida, J., Amorim, A., Bianchi, F., Breitenlechner, M., David, A., Downard, A., Dunne, E. M., Duplissy, J., Ehrhart, S., Flagan, R. C., Franchin, A., Hansel, A., Junninen, H., Kajos, M., Keskinen, H., Kupc, A., Kürten, A., Kvashin, A. N., Laaksonen, A., Lehtipalo, K., Makhmutov, V., Mathot, S., Nieminen, T., Onnela, A., Petäjä, T., Praplan, A. P., Santos, F. D., Schallhart, S., Seinfeld, J. H., Sipilä, M., Spracklen, D. V., Stozhkov, Y., Stratmann, F., Tomé, A., Tsagkogeorgas, G., Vaattovaara, P., Viisanen, Y., Virtala, A., Wagner, P. E., Weingartner, E., Wex, H., Wimmer, D., Carslaw, K. S., Curtius, J., Donahue, N. M., Kirkby, J., Kulmala, M., Worsnop, D. R., and Baltensperger, U.: Oxidation products of biogenic emissions contribute to nucleation of atmospheric particles, *Science*, 344, 717–721, <https://doi.org/10.1126/science.1243527>, 2014.
- 540 Riipinen, I., Yli-Juuti, T., Pierce, J. R., Petäjä, T., Worsnop, D. R., Kulmala, M., and Donahue, N. M.: The contribution of organics to atmospheric nanoparticle growth, *Nat. Geosci.*, 5, 453–458, <https://doi.org/10.1038/ngeo1499>, 2012.
- Shantz, N. C., Leaitch, W. R., Phinney, L., Mozurkewich, M., and Toom-Saunty, D.: The effect of organic compounds on the growth rate of cloud droplets in marine and forest settings, *Atmos. Chem. Phys.*, 8, 5869–5887, <https://doi.org/10.5194/acp-8-5869-2008>, 2008.

- 545 Sipilä, M., Berndt, T., Petäjä, T., Brus, D., Vanhanen, J., Stratmann, F., Patokoski, J., Mauldin, R. L., Hyvärinen, A.-P., Lihavainen, H., and Kulmala, M.: The role of sulfuric acid in atmospheric nucleation, *Science*, 327, 1243–1246, <https://doi.org/10.1126/science.1180315>, 2010.
- Smith, J. N., Draper, D. C., Chee, S., Dam, M., Glicker, H., Myers, D., Thomas, A. E., Lawler, M. J., and Myllys, N.: Atmospheric clusters to nanoparticles: Recent progress and challenges in closing the gap in chemical composition, *J. Aerosol. Sci.*, 153, 105733, <https://doi.org/10.1016/j.jaerosci.2020.105733>, 2021.
- 555 Stolzenburg, D., Fischer, L., Vogel, A. L., Heinritzi, M., Schervish, M., Simon, M., Wagner, A. C., Dada, L., Ahonen, L. R., Amorim, A., Baccarini, A., Bauer, P. S., Baumgartner, B., Bergen, A., Bianchi, F., Breitenlechner, M., Brilke, S., Buenrostro Mazon, S., Chen, D., Dias, A., Draper, D. C., Duplissy, J., El Haddad, I., Finkenzeller, H., Frege, C., Fuchs, C., Garmash, O., Gordon, H., He, X., Helm, J., Hofbauer, V., Hoyle, C. R., Kim, C., Kirkby, J., Kontkanen, J., Kürten, A., Lampilahti, J., Lawler, M., Lehtipalo, K., Leiminger, M., Mai, H., Mathot, S., Mentler, B., Molteni, U., Nie, W., Nieminen, T., Nowak, J. B., Ojdanic, A., Onnela, A., Passananti, M., Petäjä, T., Quéléver, L. L. J., Rissanen, M. P., Sarnela, N., Schallhart, S., Tauber, C., Tomé, A., Wagner, R., Wang, M., Weitz, L., Wimmer, D., Xiao, M., Yan, C., Ye, P., Zha, Q., Baltensperger, U., Curtius, J., Dommen, J., Flagan, R. C., Kulmala, M., Smith, J. N., Worsnop, D. R., Hansel, A., Donahue, N. M., and Winkler, P. M.: Rapid growth of organic aerosol nanoparticles over a wide tropospheric temperature range, *Proc. Natl. Acad. Sci. U.S.A.*, 115, 9122–9127, <https://doi.org/10.1073/pnas.1807604115>, 2018.
- 565 Stolzenburg, D., Simon, M., Ranjithkumar, A., Kürten, A., Lehtipalo, K., Gordon, H., Ehrhart, S., Finkenzeller, H., Pichelstorfer, L., Nieminen, T., He, X.-C., Brilke, S., Xiao, M., Amorim, A., Baalbaki, R., Baccarini, A., Beck, L., Bräkling, S., Caudillo Murillo, L., Chen, D., Chu, B., Dada, L., Dias, A., Dommen, J., Duplissy, J., El Haddad, I., Fischer, L., Gonzalez Carracedo, L., Heinritzi, M., Kim, C., Koenig, T. K., Kong, W., Lamkaddam, H., Lee, C. P., Leiminger, M., Li, Z., Makhmutov, V., Manninen, H. E., Marie, G., Marten, R., Müller, T., Nie, W., Partoll, E., Petäjä, T., Pfeifer, J., Philippov, M., Rissanen, M. P., Rörup, B., Schobesberger, S., Schuchmann, S., Shen, J., Sipilä, M., Steiner, G., Stozhkov, Y., Tauber, C., Tham, Y. J., Tomé, A., Vazquez-Pufleau, M., Wagner, A. C., Wang, M., Wang, Y., Weber, S. K., Wimmer, D., Wlasits, P. J., Wu, Y., Ye, Q., Zauner-Wieczorek, M., Baltensperger, U., Carslaw, K. S., Curtius, J., Donahue, N. M., Flagan, R. C., Hansel, A., Kulmala, M., Lelieveld, J., Volkamer, R., Kirkby, J., and Winkler, P. M.: Enhanced growth rate of atmospheric particles from sulfuric acid, *Atmos. Chem. Phys.*, 20, 7359–7372, <https://doi.org/10.5194/acp-20-7359-2020>, 2020.
- 570 Stolzenburg, D., Cai, R., Blichner, S. M., Kontkanen, J., Zhou, P., Makkonen, R., Kerminen, V.-M., Kulmala, M., Riipinen, I., and Kangasluoma, J.: Atmospheric nanoparticle growth, *Rev. Mod. Phys.*, 95, 045002, <https://doi.org/10.1103/RevModPhys.95.045002>, 2023.
- 575 Sullivan, R. C., Petters, M. D., DeMott, P. J., Kreidenweis, S. M., Wex, H., Niedermeier, D., Hartmann, S., Claus, T., Stratmann, F., Reitz, P., Schneider, J., and Sierau, B.: Irreversible loss of ice nucleation active sites in mineral dust particles caused by sulphuric acid condensation, *Atmos. Chem. Phys.*, 10, 11471–11487, <https://doi.org/10.5194/acp-10-11471-2010>, 2010.
- 580 Sun, J., Hermann, M., Weinhold, K., Merkel, M., Birmili, W., Yang, Y., Tuch, T., Flentje, H., Briel, B., Ries, L., Couret, C., Elsassler, M., Sohmer, R., Wirtz, K., Meinhardt, F., Schütze, M., Bath, O., Hellack, B., Kerminen, V.-M., Kulmala, M., Ma, N., and Wiedensohler, A.: Measurement report: Contribution of atmospheric new particle formation to ultrafine particle concentration, cloud condensation nuclei, and radiative forcing – results from 5-year observations in central europe, *Atmos. Chem. Phys.*, 24, 10667–10687, <https://doi.org/10.5194/acp-24-10667-2024>, 2024.
- 585 Surdu, M., Lamkaddam, H., Wang, D. S., Bell, D. M., Xiao, M., Lee, C. P., Li, D., Caudillo, L., Marie, G., Scholz, W., Wang, M., Lopez, B., Piedehierro, A. A., Ataei, F., Baalbaki, R., Bertozzi, B., Bogert, P., Brasseur, Z., Dada, L., Duplissy, J., Finkenzeller, H., He, X.-C., Höhler, K., Korhonen, K., Krechmer, J. E., Lehtipalo, K., Mahfouz, N. G. A., Manninen, H. E., Marten, R., Massabò, D., Mauldin, R., Petäjä, T., Pfeifer, J., Philippov, M., Rörup, B., Simon, M., Shen, J., Umo, N. S., Vogel, F., Weber, S. K., Zauner-Wieczorek, M., Volkamer, R., Saathoff, H., Möhler, O., Kirkby, J., Worsnop, D. R., Kulmala, M.,

- 590 Stratmann, F., Hansel, A., Curtius, J., Welti, A., Riva, M., Donahue, N. M., Baltensperger, U., and El Haddad, I.: Molecular understanding of the enhancement in organic aerosol mass at high relative humidity, *Environ. Sci. Technol.*, *57*, 2297–2309, <https://doi.org/10.1021/acs.est.2c04587>, 2023.
- Temelso, B., Morrell, T. E., Shields, R. M., Allodi, M. A., Wood, E. K., Kirschner, K. N., Castonguay, T. C., Archer, K. A., and Shields, G. C.: Quantum mechanical study of sulfuric acid hydration: Atmospheric implications, *J. Phys. Chem. A*, *116*, 2209–2224, <https://doi.org/10.1021/jp2119026>, 2012.
- 595 Tröstl, J., Chuang, W. K., Gordon, H., Heinritzi, M., Yan, C., Molteni, U., Ahlm, L., Frege, C., Bianchi, F., Wagner, R., Simon, M., Lehtipalo, K., Williamson, C., Craven, J. S., Duplissy, J., Adamov, A., Almeida, J., Bernhammer, A.-K., Breitenlechner, M., Brilke, S., Dias, A., Ehrhart, S., Flagan, R. C., Franchin, A., Fuchs, C., Guida, R., Gysel, M., Hansel, A., Hoyle, C. R., Jokinen, T., Junninen, H., Kangasluoma, J., Keskinen, H., Kim, J., Krapf, M., Kürten, A., Laaksonen, A., Lawler, M., Leiminger, M., Mathot, S., Möhler, O., Nieminen, T., Onnela, A., Petäjä, T., Piel, F. M., Miettinen, P., Rissanen, M. P., Rondo, L., Sarnela, N., Schobesberger, S., Sengupta, K., Sipilä, M., Smith, J. N., Steiner, G., Tomè, A., Virtanen, A., Wagner, A. C.,  
600 Weingartner, E., Wimmer, D., Winkler, P. M., Ye, P., Carslaw, K. S., Curtius, J., Dommen, J., Kirkby, J., Kulmala, M., Riipinen, I., Worsnop, D. R., Donahue, N. M., and Baltensperger, U.: The role of low-volatility organic compounds in initial particle growth in the atmosphere, *Nature*, *533*, 527–531, <https://doi.org/10.1038/nature18271>, 2016.
- Vogel, A. L., Schneider, J., Müller-Tautges, C., Phillips, G. J., Pöhlker, M. L., Rose, D., Zuth, C., Makkonen, U., Hakola, H., Crowley, J. N., Andreae, M. O., Pöschl, U., and Hoffmann, T.: Aerosol chemistry resolved by mass spectrometry: Linking  
605 field measurements of cloud condensation nuclei activity to organic aerosol composition, *Environ. Sci. Technol.*, *50*, 10823–10832, <https://doi.org/10.1021/acs.est.6b01675>, 2016.
- Wang, J., Shilling, J. E., Liu, J., Zelenyuk, A., Bell, D. M., Petters, M. D., Thalman, R., Mei, F., Zaveri, R. A., and Zheng, G.: Cloud droplet activation of secondary organic aerosol is mainly controlled by molecular weight, not water solubility, *Atmos. Chem. Phys.*, *19*, 941–954, <https://doi.org/10.5194/acp-19-941-2019>, 2019.
- 610 Wang, Z., Su, H., Wang, X., Ma, N., Wiedensohler, A., Pöschl, U., and Cheng, Y.: Scanning supersaturation condensation particle counter applied as a nano-CCN counter for size-resolved analysis of the hygroscopicity and chemical composition of nanoparticles, *Atmos. Meas. Tech.*, *8*, 2161–2172, <https://doi.org/10.5194/amt-8-2161-2015>, 2015.
- Wang, Z. B., Hu, M., Yue, D. L., Zheng, J., Zhang, R. Y., Wiedensohler, A., Wu, Z. J., Nieminen, T., and Boy, M.: Evaluation on the role of sulfuric acid in the mechanisms of new particle formation for beijing case, *Atmos. Chem. Phys.*, *11*, 12663–  
615 12671, <https://doi.org/10.5194/acp-11-12663-2011>, 2011.
- Wiedensohler, A. and Fissan, H. J.: Aerosol charging in high purity gases, *J. Aerosol Sci.*, *19*, 867–870, [https://doi.org/10.1016/0021-8502\(88\)90054-7](https://doi.org/10.1016/0021-8502(88)90054-7), 1988.
- Wiedensohler, A., Lütke-meier, E., Feldpausch, M., and Helsper, C.: Investigation of the bipolar charge distribution at various gas conditions, *Journal of Aerosol Science*, *17*, 413–416, [https://doi.org/10.1016/0021-8502\(86\)90118-7](https://doi.org/10.1016/0021-8502(86)90118-7), 1986.
- 620 Xiao, S., Wang, M. Y., Yao, L., Kulmala, M., Zhou, B., Yang, X., Chen, J. M., Wang, D. F., Fu, Q. Y., Worsnop, D. R., and Wang, L.: Strong atmospheric new particle formation in winter in urban shanghai, China, *Atmos. Chem. Phys.*, *15*, 1769–1781, <https://doi.org/10.5194/acp-15-1769-2015>, 2015.
- Yang, H., Raucchi, U., Iyer, S., Hasan, G., Golin Almeida, T., Barua, S., Savolainen, A., Kangasluoma, J., Rissanen, M., Vehkamäki, H., and Kurtén, T.: Molecular dynamics-guided reaction discovery reveals endoperoxide-to-alkoxy radical isomerization as key branching point in  $\alpha$ -pinene ozonolysis, *Nat Commun*, *16*, 661, <https://doi.org/10.1038/s41467-025-55985-w>, 2025.

- 630 Yao, L., Garmash, O., Bianchi, F., Zheng, J., Yan, C., Kontkanen, J., Junninen, H., Mazon, S. B., Ehn, M., Paasonen, P., Sipilä, M., Wang, M., Wang, X., Xiao, S., Chen, H., Lu, Y., Zhang, B., Wang, D., Fu, Q., Geng, F., Li, L., Wang, H., Qiao, L., Yang, X., Chen, J., Kerminen, V.-M., Petäjä, T., Worsnop, D. R., Kulmala, M., and Wang, L.: Atmospheric new particle formation from sulfuric acid and amines in a Chinese megacity, *Science*, 361, 278–281, <https://doi.org/10.1126/science.aao4839>, 2018.
- Yishake, J., Zang, H., Tan, R., Yao, L., Guo, S., Zhao, Y., and Li, C.: Size- and Composition-Dependent Hygroscopic Growth of Sub-20 nm Atmospherically Relevant Particles: Implications for New Particle Survival, *Environ. Sci. Technol.*, *acs.est.5c00068*, <https://doi.org/10.1021/acs.est.5c00068>, 2025.
- 635 Yu, H., Dai, L., Zhao, Y., Kanawade, V. P., Tripathi, S. N., Ge, X., Chen, M., and Lee, S.: Laboratory observations of temperature and humidity dependencies of nucleation and growth rates of sub-3 nm particles, *J. Geophys. Res.-Atmos.*, 122, 1919–1929, <https://doi.org/10.1002/2016JD025619>, 2017.
- Yuan, C., Ma, Y., Diao, Y., Yao, L., Zhou, Y., Wang, X., and Zheng, J.: CCN activity of secondary aerosols from terpene ozonolysis under atmospheric relevant conditions, *J. Geophys. Res.-Atmos.*, 122, 4654–4669, <https://doi.org/10.1002/2016JD026039>, 2017.
- 640 Zhang, K., Xu, Z., Gao, J., Xu, Z., and Wang, Z.: Review of online measurement techniques for chemical composition of atmospheric clusters and sub-20 nm particles, *Front. Environ. Sci.*, 10, 937006, <https://doi.org/10.3389/fenvs.2022.937006>, 2022.
- 645 Zhang, K., Xu, Z., Pei, X., Zhang, F., Su, H., Cheng, Y., and Wang, Z.: Characteristics of scanning flow condensation particle counter (SFPC): A rapid approach for retrieving hygroscopicity and chemical composition of sub-10 nm aerosol particles, *Aerosol Sci. Technol.*, 57, 1031–1043, <https://doi.org/10.1080/02786826.2023.2245859>, 2023.
- Zhang, K., Xiong, C., Cheng, Y., Ma, N., Mikhailov, E., Pöschl, U., Su, H., and Wang, Z.: Assessment of Hygroscopicity Uncertainties Associated With Size and Thermodynamic Model: Implications for Inferring Chemical Composition of Sub-10 nm Particles, *J. Geophys. Res.-Atmos.*, 130, e2025JD043835, <https://doi.org/10.1029/2025JD043835>, 2025.
- 650 Zhang, R., Suh, I., Zhao, J., Zhang, D., Fortner, E. C., Tie, X., Molina, L. T., and Molina, M. J.: Atmospheric new particle formation enhanced by organic acids, *Science*, 304, 1487–1490, <https://doi.org/10.1126/science.1095139>, 2004.
- Zhang, R., Wang, L., Khalizov, A. F., Zhao, J., Zheng, J., McGraw, R. L., and Molina, L. T.: Formation of nanoparticles of blue haze enhanced by anthropogenic pollution, *Proc. Natl. Acad. Sci. U.S.A.*, 106, 17650–17654, <https://doi.org/10.1073/pnas.0910125106>, 2009.
- 655 Zhang, R., Khalizov, A., Wang, L., Hu, M., and Xu, W.: Nucleation and growth of nanoparticles in the atmosphere, *Chem. Rev.*, 112, 1957–2011, <https://doi.org/10.1021/cr2001756>, 2012.
- Zhao, B., Donahue, N. M., Zhang, K., Mao, L., Shrivastava, M., Ma, P.-L., Shen, J., Wang, S., Sun, J., Gordon, H., Tang, S., Fast, J., Wang, M., Gao, Y., Yan, C., Singh, B., Li, Z., Huang, L., Lou, S., Lin, G., Wang, H., Jiang, J., Ding, A., Nie, W., Qi, X., Chi, X., and Wang, L.: Global variability in atmospheric new particle formation mechanisms, *Nature*, 631, 98–105, <https://doi.org/10.1038/s41586-024-07547-1>, 2024.
- 660 Zhao, D. F., Buchholz, A., Kortner, B., Schlag, P., Rubach, F., Fuchs, H., Kiendler-Scharr, A., Tillmann, R., Wahner, A., Watne, Å. K., Hallquist, M., Flores, J. M., Rudich, Y., Kristensen, K., Hansen, A. M. K., Glasius, M., Kourtchev, I., Kalberer, M., and Mentel, Th. F.: Cloud condensation nuclei activity, droplet growth kinetics, and hygroscopicity of biogenic and anthropogenic secondary organic aerosol (SOA), *Atmos. Chem. Phys.*, 16, 1105–1121, <https://doi.org/10.5194/acp-16-1105-2016>, 2016.

665 Zhou, R., Afsana, S., Wei, C., and Mochida, M.: Additive water uptake of the mixtures of urban atmospheric HULIS and ammonium sulfate, *J. Geophys. Res.-Atmos.*, 129, e2023JD040553, <https://doi.org/10.1029/2023JD040553>, 2024.

Zollner, J. H., Glasoe, W. A., Panta, B., Carlson, K. K., McMurry, P. H., and Hanson, D. R.: Sulfuric acid nucleation: Power dependencies, variation with relative humidity, and effect of bases, *Atmos. Chem. Phys.*, 12, 4399–4411, <https://doi.org/10.5194/acp-12-4399-2012>, 2012.

670